Monooxygenation Mechanism by Cytochrome P-450

Masayuki Hata,* Yoshinori Hirano, Tyuji Hoshino, and Minoru Tsuda

Contribution from the Laboratory of Physical Chemistry, Faculty of Pharmaceutical Sciences, Chiba University, Chiba 263-8522, Japan

Received March 14, 2000. Revised Manuscript Received April 16, 2001

Abstract: The substrate oxygenation mechanism by an ultimate species in monooxygenation by cytochrome P-450 (compound **I**) was investigated by the density functional theory method. An initial model compound was constructed from a structure obtained by 300-ps molecular dynamics simulation of compound **I**-formed P-450cam under physiologic conditions, and it consisted of porphine for protoporphyrin IX, $S^{-}-CH_3$ for the side chain of Cys357 of the fifth ligand of heme, a methane molecule for the substrate, a heme iron, and an oxygen atom of the sixth ligand of heme. The results of the calculation revealed that the substrate oxygenation mechanism had four elementary processes, i.e., (1) formation of $[FeOH]^{3+}$ and a substrate radical by hydrogen atom abstraction from the substrate caused by $[FeO]^{3+}$, (2) rotation of the OH group of the sixth ligand of $[FeOH]^{3+}$ produced by process 1, (3) substrate radical binding with the $[FeOH]^{3+}$, and (4) elimination of the oxygenated substrate formed at the sixth ligand binding site. The rate-determining step is process 1, hydrogen atom abstraction from the substrate, and the activation energy was determined to be about 15 kcal/mol. For this reason, it is thought that this reaction occurs in vivo.

1. Introduction

Cytochrome P-450s are widely distributed among various forms of life, including animals, plants, and microorganisms, and play vital roles in normal metabolism.[1] It is well-known that binding of a substrate to ferric cytochrome P-450 initiates the so-called monooxygenation reaction cycle.[2] Introduction of the first electron to substrate-bound cytochrome P-450 reduces ferric heme to a ferrous form to obtain an oxygen molecule. The second electron is introduced to oxygenated heme, resulting in activation of the bound oxygen molecule, and an oxygen atom attaches to the substrate.[1−4] That is to say, splitting of the O−O bond of the activated oxygen molecule occurs to oxygenate the substrate, but the reaction is too rapid to observe the reaction intermediates.[4] Thus, the reaction mechanism remains unclear.

Traditionally, mechanistic studies of substrate monooxygenation by cytochrome P-450 have been based on the concept of the two successive processes: the formation process of the ultimate species for monooxygenation, $[FeO]^{3+}$ (compound **I**), and the monooxygenation process of a substrate by the ultimate species.[4] Harris et al. clarified theoretically the first step using the density functional theory (DFT) method and showed the electronic structure of compound **I**.[5] However, the monooxygenation process of the substrate by $[FeO]^{3+}$ remains unclear. In this study, we investigated the monooxygenation process of substrates by cytochrome P-450 by means of theoretical calculation.

2. Methods

2.1. Molecular Dynamics Simulation. First of all, molecular dynamics (MD) simulations were performed to determine the structure of the ultimate species $[FeO]^{3+}$ in the enzyme.

2.1.1. Construction of the Model for Calculation. Poulos et al. determined the 3-D structure of the substrate (*d*-camphor)-bound cytochrome P-450cam from *Pseudomonas putida*[6] and registered it in the Protein Data Bank (PDB,[7−9] pdbcode: 2cpp). This structure was used for our investigation of the monooxygenation mechanism by cytochrome P-450. The model for the MD simulation was constructed in the following way. A sphere of water molecules (TIP3P model[10]) was generated by the Monte Carlo method,[11] and the center of the sphere corresponded to the heme Fe atom of the substrate-bound P-450cam. The radius of the sphere was 25 Å, and there were 1824 water molecules in the model.

2.1.2. Computational Details. MD simulation is performed by solving Newton's equation of motion (eq 1), which propagates a time-sequence of changes of all position vectors of N atoms involved in a molecular system:

$$m_i \mathrm{d}^2 r_i(t)/\mathrm{d}t^2 = -\partial V\{r_1(t), r_2(t), ..., r_N(t)\}/\partial r_i(t) \qquad (1)$$

where $-\partial V\{r_1(t), r_2(t), ..., r_N(t)\}$ is the potential energy function

(1) Omura, T. *Cytochrome P-450,* 2nd ed.; Omura, T., Ishimura, Y., Fujii-Kuriyama, Y., Eds.; Kodansha: Tokyo, 1993; pp 1−15.

(2) Estabrook, R. W.; Hildebrandt, A. G.; Baron, J.; Netter, K. J.; Leibman, K. *Biochem. Biophys. Res. Commun.* **1971**, *42*, 132−139.

(3) Imai, M.; Shimada, H.; Watanabe, Y.; Matsushita-Hibiya, Y.; Makino, R.; Koga, H.; Horiuchi, T.; Ishimura, Y. *Proc. Natl. Acad. Sci. U.S.A.* **1989**, *86*, 7823−7827.

(4) Ishimura, Y. *Cytochrome P-450,* 2nd ed.; Omura, T., Ishimura, Y., Fujii-Kuriyama, Y., Eds.; Kodansha: Tokyo, 1993; pp 80−91.

(5) Harris, D. L.; Loew, G. H. *J. Am. Chem. Soc.* **1998**, *120*, 8941−8948.

(6) Poulos, T. L.; Finzel, B. C.; Howard, A. J. *J. Mol. Biol.* **1987**, *195*, 687−700.

(7) Bernstein, F. C.; Koetzle, T. F.; Williams, G. J. B.; Meyer, E. F., Jr.; Brice, M. D.; Rodgers, J. R.; Kennard, O.; Shimanouchi, T.; Tasumi, M. *J. Mol. Biol.* **1977**, *112*, 535−542.

(8) Abola, E. E.; Bernstein, F. C.; Bryant, S. H.; Koetzle, T. F.; Weng, J. Protein Data Bank. In *Crystallographic Databases−Information Content, Software Systems, Scientific Applications*; Allen, F. H., Bergerhoff, G., Sievers, R., Eds.; Data Commission of the International Union of Crystallography: Bonn/Cambridge/Chester, 1987; pp 107−132.

(9) Abola, E. E.; Manning, N. O.; Prilusky, J.; Stampf, D. R.; Sussman, J. L. *J. Res. Natl. Inst. Stand. Technol.* **1996**, *101*, 231−241.

(10) Jorgensen, W. L.; Chandrasekhar, J.; Madura, J. D. *J. Chem. Phys.* **1983**, *79*, 926−935.

(11) Pearlman, D. A.; Case, D. A.; Caldwell, J. W.; Ross, W. S.; Cheatham, T. E., III; Ferguson, D. M.; Seibel, G. L.; Singh, U. C.; Weiner, P. K.; Kollman, P. A. *AMBER 4.1*; University of California: San Francisco, 1995.

10.1021/ja000908p CCC: $20.00
Published on Web 06/12/2001

of the molecular system, $r_i(t)$ is the position vector of the ith atom at time t, m_i is the mass of the ith atom, and $-\partial V/\partial r_i(t)$ is the force that acts on the ith atom. The computational program used was AMBER 4.1.[11] A united-atom force field[12] was applied to the model structure except for *d*-camphor, for which an all-atom force field[13] was used.

Point charges on heme, compound **I**, and *d*-camphor for use in MD simulations were determined using density functional theory (DFT) calculation.[14] Local density approximation (LDA) was used to calculate exchange and correlation energies. The functionals used were the Hedin−Lundqvist/Janak−Morruzi−Williams local correlation functionals (JMW). The basis set used was the double-numeric quality basis set with polarization functions (DNP), which corresponds to Gaussian 6-31G** basis sets.[15] Because of the large numbers of electrons in the models for calculations, a frozen core approximation was applied to 1s electrons of carbon, nitrogen, and oxygen atoms as well as 1s, 2s, 3s, 3p electrons of an Fe atom. Heme and *d*-camphor models for the calculations were constructed by extracting each corresponding part from the substrate-bound P-450cam structure,[6] whereas the substrate-free P-450cam structure (pdbcode: 1phc)[16] was used for construction of the compound **I** model because the positions of heme Fe atoms differ in the two structures. The fifth ligand of heme and compound **I** models was S^--CH_3. The structure at the sixth ligand of compound **I** on the potential energy hypersurface was more-precisely fully optimized. Other atoms were fixed in the extracted model structures. The spin multiplicities were sextet for heme, doublet for compound **I**, and singlet for *d*-camphor. The total atomic charge was 0 e. The computational program used was DMol 96.0.[15] For point charges on the other residues, the standard AMBER residue database was utilized. For vdW parameters, the AMBER Force Field Parameter File was utilized.

The MD simulation proceeded in the following way. The structure of the model, as described in the previous section, was fully energy-minimized after energy-minimization on the water molecules using the BELLY option.[17] Using the energy-minimized structure, 34-ps MD simulation for heating was performed with a time step of 0.002 ps. The process is as follows: (1) MD simulation on the water molecules at 5 K for 6 ps, (2) MD simulation on all of the atoms of the system at 5 K for 4 ps, and (3) MD simulation on all of the atoms of the system at 50 K for 4 ps. After this calculation, the temperature of the system was increased 50 K for every 4-ps MD simulation, i.e., 100 K, 150 K, ..., 300 K.

After the heating process, the MD simulation was performed at 310 K for 300 ps with a time step of 0.002 ps. The trajectory at that temperature (310 K for 300 ps) was considered to be the most probable structure under physiologic conditions, and the average structure in the 300-ps MD simulation was obtained.

Calculations of the nonbonded term in the MD simulations were accelerated by the use of a hardware accelerator called an MD Engine,[18] which has a special processor chip, MODEL, to calculate the nonbonded term. A cutoff distance (8 Å) was applied for computation of van der Waals forces (r^{-6} and r^{-12}). The electrostatic term (r^{-1}) was calculated with no cutoff, taking full advantage of the MD Engine, because simplification in the computation of this term causes a noticeable error. The SHAKE constraint,[19] where all of the bonds are kept at equilibrium distances, was used. The water molecules were restricted within the sphere by a soft harmonic potential for which the force constant was 1.5 kcal/Å.

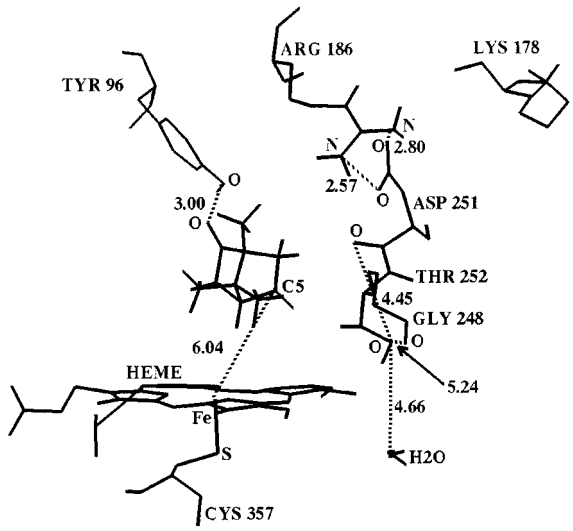

Figure 1. Active site of the substrate-bound P-450cam obtained by MD simulation at 310 K. Numerals are interatomic distances in Å.

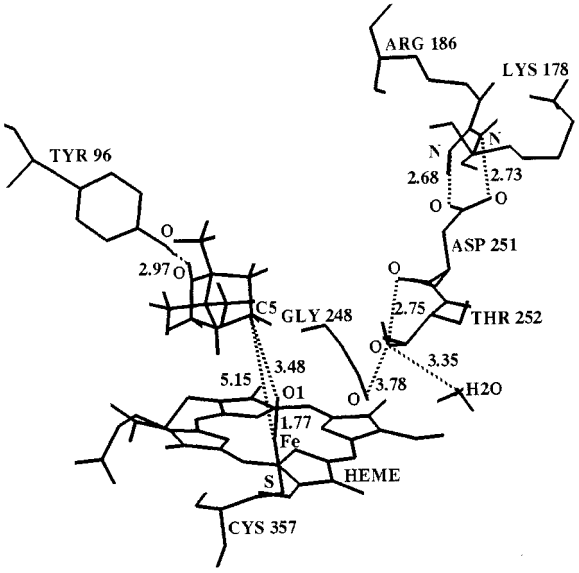

Figure 2. Active site of the currently believed ultimate species (compound **I**) obtained by MD simulation at 310 K. Numerals are interatomic distances in Å.

According to the above-described procedure, MD simulations were performed on both a substrate-bound ferric P-450cam and a compound **I**-formed one. The results are shown in Figures 1 and 2.

2.2. Quantum Mechanics Calculation Using the DFT Method. Using the ultimate species $[FeO]^{3+}$ structure obtained by the above-mentioned method, the process of monooxygenation by cytochrome P-450 was investigated in detail by means of the DFT method.

(12) Weiner, S. J.; Kollman, P. A.; Case, D. A.; Singh, U. C.; Ghio, C.; Alagona, G.; Profeta, S., Jr.; Weiner, P. *J. Am. Chem. Soc.* **1984**, *106*, 765−784.

(13) Weiner, S. J.; Kollman, P. A.; Nguyen, D. T.; Case, D. A. *J. Comput. Chem.* **1986**, *7*, 230−252.

(14) Hata, M.; Nishida, R.; Ohmori, N.; Tsuda, M. *JCPE J.* **2000**, *12*, 195−202.

(15) *DMol*, Version 96.0; Molecular Simulations, Inc.: San Diego, 1996.

(16) Poulos, T. L.; Funzel, B. C.; Howard, A. J. *Biochemistry* **1986**, *25*, 5314−5322.

(17) Brown, F. K.; Kollman, P. A. *J. Mol. Biol.* **1987**, *198*, 533−546.

(18) Toyoda, S.; Miyagawa, H.; Kitamura, K.; Amisaki, T.; Hashimoto, E.; Ikeda, H.; Kusumi, A.; Miyakawa, N. *J. Comput. Chem.* **1999**, *20*, 185−199.

(19) Ryckaert, J.; Ciccotti, G.; Berendsen, H. J. C. *J. Comput. Phys.* **1977**, *23*, 327−341.

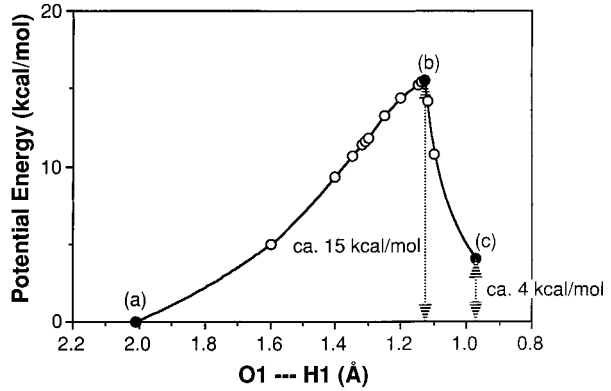

Figure 3. Potential energy change following hydrogen atom abstraction from the substrate by compound **I**. Horizontal and vertical axes represent the distance between O1 and H1 atoms (Å) and the potential energy change (kcal/mol), respectively.

2.2.1. Construction of Models for Calculation. Heme, its ligands, and *d*-camphor, which are considered to participate directly in the monooxygenation process, were extracted to construct models for the DFT study. The protoporphyrin IX part of heme and the side chain of Cys357 at the fifth ligand binding site were replaced with porphine and $S^{-}-CH_3$, respectively. D-Camphor was changed into a methane molecule, i.e., C4, C5, and C6 atoms and two hydrogen atoms bonding a C5 atom were extracted, and C4 and C6 atoms were replaced with hydrogen atoms. The constructed models are shown in Figures 4, 6, and 8.

2.2.2. Computational Details. The Schrödinger equations of the model compounds were solved by using the DFT method. The basis set used was 3-21G**. The exchange functional was Becke's three-parameter functional,[20] and the correlation functional was Lee−Yang−Parr's formula.[21] The structures at the minima on the substrate, the sixth ligand of heme, heme iron, and sulfur atom of the fifth ligand on the potential energy hypersurface were more-precisely fully optimized. Other atoms were fixed in the structure obtained by MD simulation (Figure 2). Potential energy profiles were obtained by changing parameters shown in horizontal axes of Figures 3, 5, and 7. For this reason, values of activation energy and heat of formation were described in integers. The computational program used was Gaussian 98.[22]

Some studies on the stable spin state of compound **I** have been carried out using the DFT method. Harris et al. calculated the structures of compound **I** using the DGauss 4.0 program.[23] The exchange and correlation functionals used were Becke's 1988 functional[24] and the Perdew−Wang 1991[25] gradient-corrected correlation functional, and the basis set used was a double-ζ valence polarization DGauss basis set (DZVP). The results showed that the potential energy of the doublet state was 3 kcal/mol lower than that of the quartet state.[5] On the other hand, Filatov et al. used the CADPAC5 program[26] and performed calculations using the BP86 density functional [24,27] with several basis sets. It was found that the doublet state was slightly higher in energy than the quartet state.[28] They proposed a two-state reactivity (TSR) mechanism, i.e., in the hydroxylation of the substrate by P-450 ferryl complex, spin-state crossing occurs between high-spin (quartet) and low-spin (doublet) states, and a low-spin state structure is produced.[29] Our calculations showed that the potential energy of the low-spin state ($^2A_{2u}$) structure was 2.4 kcal/mol lower than that of the high-spin state ($^4A_{2u}$), agreeing with the results of Harris et al. Hence, the calculations in this study were performed at the doublet state. The total atomic charge was 0 e.

2.2.3. Evaluation of the Effect of the Dielectric Constant in Protein. Since the active site in a protein is not isolated but enclosed by many molecules or residues, the inclusion of the effect of the dielectric constant seems to be important when attempting to reproduce the environment inside the protein through theoretical approaches. Simonson et al. estimated the dielectric constant in protein to be 2−4.[30] However, Antosiewicz et al. reported that the value of pK_a for ionized groups in protein was correctly calculated using a dielectric constant of 20.[31] Furthermore, an investigation by Sham et al. indicated that the effective dielectric constant needed to be fairly high for appropriate evaluation of the interaction of electric charges in protein.[32] In this work, geometry optimizations were also performed for the stable and the transition states on the reaction path taking the dielectric constant of the surroundings to be 20. The Self-Consistent Reaction Field (SCRF) method using the Polarized Continuum Model (PCM) of Tomasi and coworkers[33−41] was used for computations with a dielectric constant of 20.

3. Results and Discussion

3.1. Dynamic Structures of a Substrate-Bound Ferric P-450cam. The dynamic structure of a substrate-bound P-450cam

(20) Becke, A. D. *J. Chem. Phys.* **1993**, *98*, 5648−5652.
(21) Lee, C.; Yang, W.; Parr, R. G. *Phys. Rev.* **1988**, *B37*, 785−789.
(22) Frisch, M. J.; Trucks, G. W.; Schlegel, H. B.; Scuseria, G. E.; Robb, M. A.; Cheeseman, J. R.; Zakrzewski, V. G.; Montgomery, J. A., Jr.; Stratmann, R. E.; Burant, J. C.; Dapprich, S.; Millam, J. M.; Daniels, A. D.; Kudin, K. N.; Strain, M. C.; Farkas, O.; Tomasi, J.; Barone, V.; Cossi, M.; Cammi, R.; Mennucci, B.; Pomelli, C.; Adamo, C.; Clifford, S.; Ochterski, J.; Petersson, G. A.; Ayala, P. Y.; Cui, Q.; Morokuma, K.; Malick, D. K.; Rabuck, A. D.; Raghavachari, K.; Foresman, J. B.; Cioslowski, J.; Ortiz, J. V.; Baboul, A. G.; Stefanov, B. B.; Liu, G.; Liashenko, A.; Piskorz, P.; Komaromi, I.; Gomperts, R.; Martin, R. L.; Fox, D. J.; Keith, T.; Al-Laham, M. A.; Peng, C. Y.; Nanayakkara, A.; Gonzalez, C.; Challacombe, M.; Gill, P. M. W.; Johnson, B.; Chen, W.; Wong, M. W.; Andres, J. L.; Gonzalez, C.; Head-Gordon, M.; Replogle, E. S.; Pople, J. A. *Gaussian 98*, revision A.7; Gaussian, Inc.: Pittsburgh, PA, 1998.
(23) *DGauss 4.0*; Oxford Molecular: Beaverton, OR.
(24) Becke, A. D. *Phys. Rev. A* **1988**, *38*, 3098−3100.
(25) Perdew, J. P.; Wang, Y. *Phys. Rev. B* **1992**, *45*, 13244−13249.
(26) Amos, R. D.; Alberts, I. L.; Andrews, J. S.; Collwell, S. M.; Handy, N. C.; Jayatilaka, D.; Knowles, P. J.; Kobayashi, R.; Koga, N.; Laidig, K. E.; Maslen, P. E.; Murray, C. W.; Rice, J. E.; Sanz, J.; Simandrias, E. D.; Stone, A. J.; Su, M.-D. *CADPAC5*; The Cambridge Analytic Derivatives Package: Cambridge, UK, 1992.
(27) Perdew, J. P. *Phys. Rev. B* **1986**, *33*, 8822−8824.
(28) Filatov, M.; Harris, N.; Shaik, S. *J. Chem. Soc., Perkin Trans. 2* **1999**, 399−410.
(29) Shaik, S.; Filatov, M.; Schröder, D.; Schwarz, H. *Chem. Eur. J.* **1998**, *4*, 193−199.
(30) Simonson, T.; Perahia, D.; Brnger, A. T. *Biophys. J.* **1991**, *59*, 670−690.
(31) Antosiewicz, J.; McCammon, J. A.; Gilson, M. K. *Biochemistry* **1996**, *35*, 7819−7833.
(32) Sham, Y. Y.; Muegge, I.; Warshel, A. *Biophys. J.* **1998**, *74*, 1744−1753.
(33) Miertus, S.; Scrocco, E.; Tomasi, J. *Chem. Phys.* **1981**, *55*, 117−129.
(34) Miertus, S.; Tomasi, J. *Chem. Phys.* **1982**, *65*, 239−245.
(35) Cossi, M.; Barone, V.; Cammi, R.; Tomasi, J. *Chem. Phys. Lett.* **1996**, *255*, 327−335.
(36) Cancès, E.; Mennucci, B.; Tomasi, J. *J. Chem. Phys.* **1997**, *107*, 3032−3041.
(37) Barone, V.; Cossi, M.; Tomasi, J. *J. Chem. Phys.* **1997**, *107*, 3210−3221.
(38) Cossi, M.; Barone, V.; Mennucci, B.; Tomasi, J. *Chem. Phys. Lett.* **1998**, *286*, 253−260.
(39) Barone, V.; Cossi, M.; Tomasi, J. *J. Comput. Chem.* **1998**, *19*, 404−417.
(40) Barone, V.; Cossi, M. *J. Phys. Chem. A* **1998**, *102*, 1995−2001.
(41) (a) Cancès, E.; Mennucci, B. *J. Chem. Phys.* **1998**, *109*, 249−259. (b) Cancès, E.; Mennucci, B.; Tomasi, J. *J. Chem. Phys.* **1998**, *109*, 260−266.

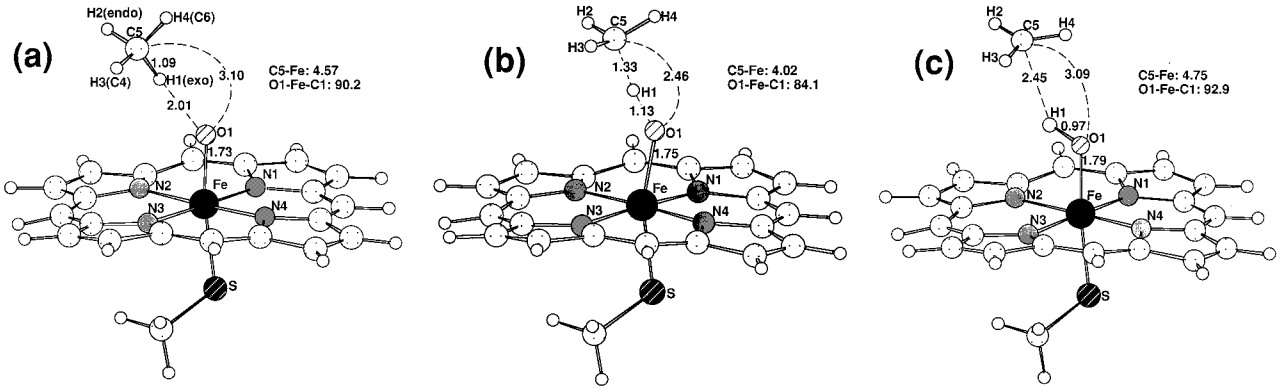

Figure 4. Structural changes following hydrogen atom abstraction from the substrate by compound **I**. Structures **a**−**c** correspond to the letters in Figure 3. Numerals are interatomic distances in Å, but those of O1−Fe−C1 are angles in deg.

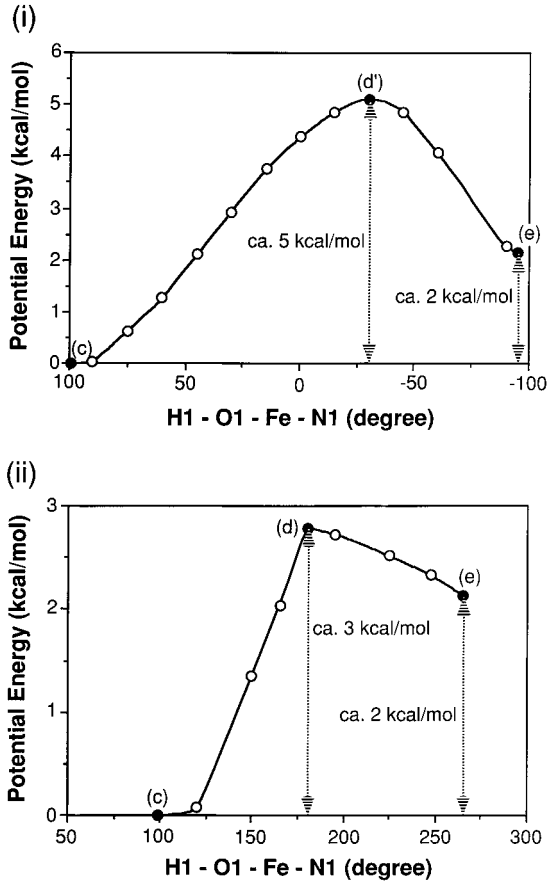

Figure 5. Potential energy change following rotation of the OH group of the sixth ligand of heme: (i) right-handed rotation and (ii) left-handed rotation. Horizontal and vertical axes represent the dihedral angle H1−O1−Fe−N1 (deg) and the potential energy change (kcal/mol), respectively.

that was obtained by MD simulation at 310 K is shown in Figure 1. It is well-known that P-450cam from *Pseudomonas putida* monooxygenates the C5 atom of *d*-camphor specifically and produces only 5-*exo*-hydroxycamphor.[42] The distance between the heme Fe atom and C5 atom of *d*-camphor increased to 5 to 6 Å from the initial value of 4.21 Å at the crystal structure[6] by 300-ps MD simulation. It should be noted that the hydrogen bond between the OH group of Tyr96 and carbonyl oxygen of *d*-camphor (see Figure 1) was maintained at about 3 Å throughout the MD simulations, although the space surrounded by the substrate (*d*-camphor) and heme increased from 4.21 Å in the crystal to 5 to 6 Å. An oxygen molecule could easily enter into this space. Hydrogen bonds between Arg186 and Asp251 and between Gly248 and Thr252 were maintained in the same way as observed in the crystal structure[6] during the MD simulation.

Introduction of the first electron to the substrate-bound cytochrome P-450 reduces ferric heme to a ferrous form to obtain an oxygen molecule. Upon receiving the second electron in the monooxygenation reaction cycle of P-450, the final step proceeds very rapidly to produce reaction products. For this reason, the mechanism of the O−O bond cleavage, as well as that of transfer of an oxygen atom to the substrate, remains unclear. However, because an active species, compound **I**, that produces such monooxygenated products in P-450 catalysis was prepared,[43] compound **I** produced in P-450 via a reaction of the oxygen molecule with two protons is currently believed to be the ultimate active species.[4] An active site of the structure obtained by the MD simulation is shown in Figure 2. The distance between the heme Fe atom and C5 atom of the substrate and the hydrogen bond distance between the OH group of Tyr96 and the carbonyl group of *d*-camphor were maintained at the same values as those shown in Figure 1. The distance between the C5 atom of the substrate and an oxygen atom, denoted O1, of the sixth ligand was maintained at the value of 3.0 to 3.5 Å during 300 ps at 310 K. As regards the two hydrogen atoms bonding a C5 atom, the distance between *exo* hydrogen and O1 atoms was 2.5 to 3.0 Å (2.95 Å in Figure 2), whereas the distance between *endo* hydrogen and O1 atoms was 3.2 to 3.7 Å (3.40 Å in Figure 2). The *exo* hydrogen atom was always the nearest from the O1 atom in the ultimate species.

3.2. Monooxygenation Mechanism by Compound I. 3.2.1. Hydrogen Atom Abstraction by Compound I. A model compound was constructed from the structure shown in Figure 2 by the procedure described in the Methods section. The optimized structure of the compound is shown in Figure 4a. An oxygen atom at the sixth ligand binding site of heme (O1) interacted with a C5 atom of the substrate (3.10 Å) and bonded a heme iron (Fe, 1.73 Å), almost corresponding to the results of MD simulation for the full structure of P-450cam (3.48 and 1.77 Å, respectively (Figure 2)). On the other hand, the distances between C5 and Fe atoms and between O1 and *exo* hydrogen (H1) atoms were 4.57 and 2.01 Å, respectively, which are much shorter than those shown in Figure 2. This result shows that the compound is ready for monooxygenation. The spin density distribution of structure **a** is shown in Table 1. It was found

(42) White, R. E.; McCarthy, M.-B.; Egeberg. K. D.; Sligar, S. G. *Arch. Biochem. Biophys.* **1984**, *228*, 493−502.

(43) White, R. E.; Coon, M. J. *Annu. Rev. Biochem.* **1980**, *49*, 315−356.

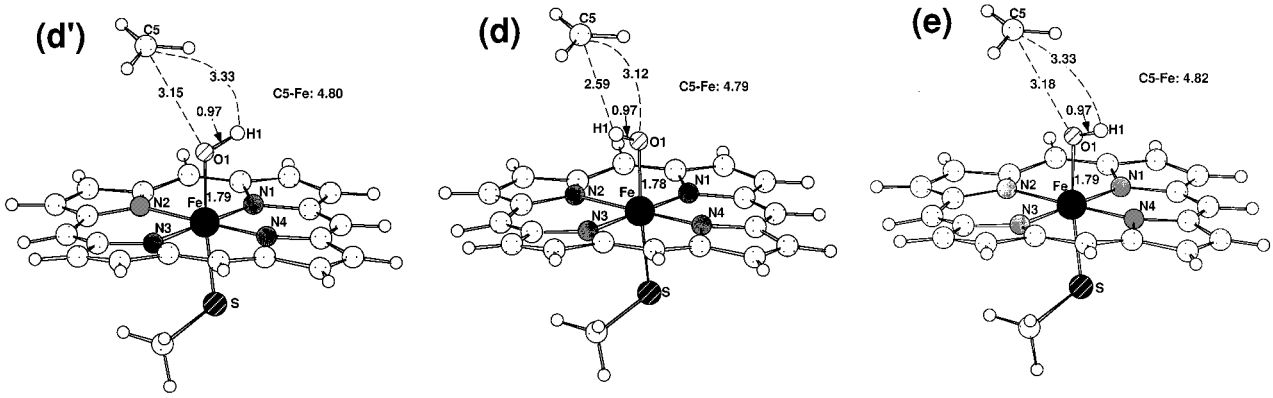

Figure 6. Structural changes following rotation of the OH group of the sixth ligand of heme. Structures **d′**, **d**, and **e** correspond to the letters in Figure 5. See Figure 4 for details of structure **c**. Numerals are interatomic distances in Å.

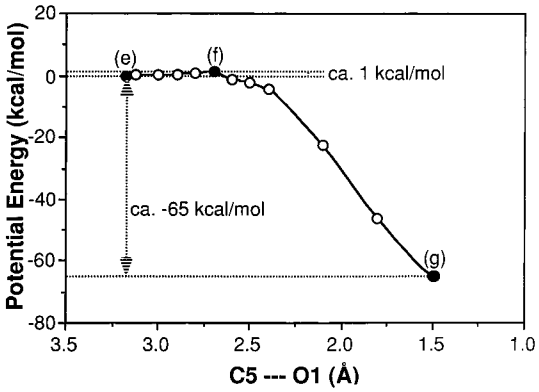

Figure 7. Potential energy change following binding reaction between the substrate and the OH group. Horizontal and vertical axes represent the distance between O1 and C5 atoms (Å) and the potential energy change (kcal/mol), respectively.

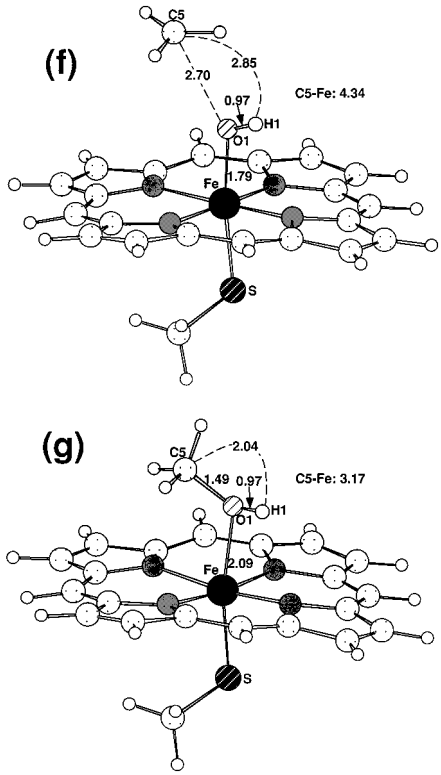

Figure 8. Structural changes following binding reaction between the substrate and the OH group. Structures **f** and **g** correspond to the letters in Figure 7. See Figure 6 for details of structure **e**. Numerals are interatomic distances in Å.

that the O1 atom of $[FeO]^{3+}$ had the character of a free radical. Harris et al. calculated the spin density distribution of $[FeO]^{3+}$ without the interaction with the substrate, and they showed that the spin density of O1 was large (0.92).[5] Our results agree with their results in the viewpoint of having the character of a free radical.

Because it is well-known that a free radical abstracts a hydrogen atom from hydrocarbons,[44] it is thought that the monooxygenation mechanism by compound **I** is initiated by *exo* hydrogen atom abstraction from the substrate, interacting with the O1 atom. Potential energy, structure, and spin density changes following the reaction are shown in Figures 3 and 4 and in Table 1, respectively. When the distance between O1 and H1 atoms decreased, potential energy increased, and then a transition state (TS) structure appeared (Figure 4b). In this structure, the distance between C5 and H1 atoms increased from an initial value of 1.09 Å to 1.33 Å, whereas the distance between C5 and O1 atoms decreased remarkably from 3.10 Å to 2.46 Å. The O1−H1 distance also decreased remarkably from 2.01 Å to 1.13 Å, while the distance between Fe and O1 atoms increased slightly from 1.73 Å to 1.75 Å. The Fe−O1 bond collapsed as the H1 atom approached the O1 atom. It can be seen that the O1−Fe−C1 angle changed from 90.2° in structure **a** to 84.1° in structure **b**. The spin density distribution (Table 1) indicates that the substrate has the character of a radical with movement of the H1 atom. Passing the TS, the sixth ligand became an OH group and the spin density localized at the substrate radical (Figure 4c and Table 1). The distance between H1 and C5 atoms increased to 2.45 Å, and the distances between C5 and O1 atoms (3.09 Å) and between C5 and Fe atoms (4.75 Å) increased again to the initial values. The O1−Fe−C1 angle (92.9°) also became nearly the same as the initial value. The distance between Fe and O1 atoms increased further (1.79 Å). The activation energy for this reaction was about 15 kcal/mol.

To check the influence of the electric constant in protein, the structures and the potential energies of structures **a**, **b**, and **c** have also been evaluated by the SCRF with the value of the dielectric constant set at 20. However, no significant differences were noticed between the results obtained from the evaluation using a dielectric constant of 1 and those obtained using a dielectric constant of 20.[45]

3.2.2. Rotation of the OH Group at the Sixth Ligand Binding Site. The C5 atom of the substrate must bond with

(44) For example, see: (a) Tomoda, Y.; Tsuda, M. *Nature* **1961**, *190*, 905. (b) Tomoda, Y.; Tsuda, M. *J. Polym. Sci.* **1961**, *54*, 321−328. (c) Morrison, R. T.; Boyd, R. N. *Organic Chemistry*, 5th ed.; Allyn and Bacon, Inc.: Newton, MA, 1987; Chapter 15.

Table 1. Spin Density Changes Following Hydrogen Atom Abstraction from the Substrate by Compound **I**[a]

groups of atoms		structures **a**	**b**	**c**
model of P-450	O1	0.42	0.43	−0.15
	Fe	−0.21	−0.08	−0.13
	Cys (S−CH_3)	0.68	0.21	0.32
	(S of Cys)	(0.49)	(0.22)	(0.32)
	porphine	0.11	0.00	−0.02
model of substrate	CH_3 (C5 + H2 + H3 + H4)	0.01	0.49	0.96
	(C5 of CH_3)	(0.01)	(0.55)	(1.13)
	H1	−0.00	−0.06	0.01
$\langle S^2 \rangle$		0.85	0.78	0.80

[a] $\langle S^2 \rangle$ values are also shown in the table. See Figure 4 for details of structures **a**, **b**, and **c**. Porphine is the rest of the model of P-450, obtained by excluding O1, Fe, and Cys. Because the spin multiplicity is a doublet, the sum of the spin densities in the structures (except for the values in parentheses) is unity. It was found in structure **a** that the O1 atom of $[FeO]^{3+}$ had the character of a free radical. Because it is well-known that a free radical abstracts a hydrogen atom from hydrocarbons,[44] it is thought that the monooxygenation mechanism by compound **I** is initiated by *exo* hydrogen atom (H1 atom) abstraction from the substrate, interacting with the O1 atom. The table indicates that the substrate has the character of a radical with movement of the H1 atom. Passing the TS (structure **b**), the spin density localized at the substrate radical (structure **c**).

the oxygen atom at the sixth ligand binding site (O1) to produce a monooxygenated substrate from the product of hydrogen atom abstraction, which was described in the previous section. Seeing the product of the abstraction, however, one can realize that a hydrogen atom from the *exo* hydrogen atom of the substrate (H1) exists between C5 and O1 atoms (Figure 4c). In an actual enzyme, the substrate is restricted in its movement due to retention by an OH group of the side chain of Tyr 96. We therefore considered that it is necessary for C5 and O1 bonding to rotate the Fe−O1 bond, i.e., the interaction between C5 and H1 atoms is cut by rotation of the OH group at the sixth ligand binding site, and a configuration that is able to bond C5 and O1 atoms is formed. Moreover, as rotation of the OH group, we investigated both right- and left-handed rotations from the sixth ligand binding site. First, potential energy, structure, and spin density changes following right-handed rotation of the OH group are shown in Figures 5i and 6 and in Table 2, respectively. When the OH group rotated in a rightward direction from an initial H1−O1−Fe−N1 dihedral angle of 99.3°, the potential energy increased, and then a TS structure appeared at the dihedral angle of −30° (Figure 6d′). The distance between C5 and H1 atoms increased from an initial value of 2.45 Å to 3.33 Å. Passing the TS, the OH group further rotated until the opposite side of the substrate existing side from the Fe−O1 bond axis, and a stable structure was obtained (Figure 6e). The activation energy for this reaction was about 5 kcal/mol.

Second, potential energy, structure, and spin density changes following a left-handed rotation of the OH group are shown in Figures 5ii and 6 and in Table 2, respectively. When the OH group rotated in a leftward direction, the potential energy increased, and then a TS structure appeared at the dihedral angle of 180° (Figure 6d). The distance between C5 and H1 atoms increased from an initial value of 2.45 Å to 2.59 Å. Passing the TS, the same process as that in the right-handed rotation occurred, and a stable structure was obtained (Figure 6e). The activation energy for this reaction was about 3 kcal/mol.

Table 2. Spin Density Changes Following Rotation of the OH Group of the Sixth Ligand of Heme[a]

groups of atoms		structures **c**	**d** **d′**	**e**
model of P-450	O1	−0.15	0.12 0.12	−0.18
	H1	0.01	−0.01 −0.01	0.01
	Fe	−0.13	−0.15 −0.30	−0.11
	Cys (S−CH_3)	0.32	0.06 0.24	0.32
	(S of Cys)	(0.32)	(0.06) (0.25)	(0.32)
	porphine[b]	−0.02	−0.00 −0.03	−0.02
model of substrate	CH_3 (C5 + H2 + H3 + H4)	0.96	0.98 0.98	0.98
	(C5 of CH_3)	(1.13)	(1.14) (1.14)	(1.14)
$\langle S^2 \rangle$		0.80	0.80 0.81	0.80

[a] $\langle S^2 \rangle$ values are also shown in the table. See Figure 4 for details of structure **c** and Figure 6 for details of structures **d**, **d′**, and **e**. Because the spin multiplicity is a doublet, the sum of the spin densities in the structures (except for the values in parentheses) is unity. Also see the footnote for Table 1. The spin density distribution did not change remarkably in both reactions (**c** → **d** → **e** and **c** → **d′** → **e**). [b] See the footnote for Table 1.

Based on a comparison of both activation energies, it is concluded that left-handed rotation occurs more easily than does right-handed rotation. This is because the substrate is located on the N1−N2 side from the Fe atom (the inner side of each structure), and it is thought that it is more difficult for interaction between the OH group and the substrate to be cut by right-handed rotation than by left-handed rotation. This is obvious from the change in the dihedral angle from structure **c** until the TS structure, i.e., the change in the right-handed rotation (ca. 130°, Figure 5i) was larger than that in the left-handed rotation (ca. 80°, Figure 5ii). The structure and spin density distribution, except for the C5−H1 distance, did not change remarkably in either reaction (Figure 6 and Table 2). Although the SCRF calculations were carried out in a similar manner with the value of the dielectric constant set at 20, no significant differences were observed between the results of these calculations and those of calculations performed using a dielectric constant of 1.[45]

3.3.3. An Oxygen Atom Insertion to the Substrate. Because O1 and C5 atoms can face each other directly and interact (3.18 Å, Figure 6e) by rotation of the OH group at the sixth ligand binding site, the rest is only binding of both atoms. Potential energy, structure, and spin density changes following the reaction are shown in Figures 7 and 8 and in Table 3, respectively. When the distance between O1 and C5 atoms decreased, the potential energy increased slightly, and then a TS structure appeared at the distance of 2.70 Å (Figure 8f). Passing the TS, the O1−C5 distance further decreased, and finally, an O1−C5 bond formed and the potential energy was stabilized (Figure 8g). The O1−C5 distance became 1.49 Å, and the distance between Fe and O1 atoms increased from the initial value of 1.79 Å to 2.09 Å. It was found by spin density changes (Table 3) that the spin density became localized at the Fe atom in structure **g** but localized at the substrate in structure

(45) Hirano et al. investigated a mechanism of phosphorylation catalyzed by cAMP-dependent protein kinase using the SCRF method, and reported that no significant differences were observed between the results of calculations using a dielectric constant of 20 and those of calculations using a dielectric constant of 1. See: Hirano, Y.; Hata, M.; Hoshino, T.; Tsuda, M. *JCPE J.* **2000**, *12*, 119−128.

Table 3. Spin Density Changes Following Binding Reaction between the Substrate and the OH Group[a]

groups of atoms		structures		
		e	**f**	**g**
model of substrate	CH_3 (C5 + H2 + H3 + H4)	0.98	0.94	−0.00
	(C5 of CH_3)	(1.14)	(1.10)	(−0.00)
	O1	−0.18	−0.20	−0.00
	H1	0.01	0.02	0.00
model of P-450	Fe	−0.11	−0.03	1.07
	Cys (S−CH_3)	0.32	0.31	0.02
	(S of Cys)	(0.32)	(0.31)	(0.02)
	porphine[b]	−0.02	−0.02	−0.10
$\langle S^2 \rangle$		0.80	0.81	0.75

[a] $\langle S^2 \rangle$ values are also shown in the table. See Figure 6 for details of structure **e** and Figure 8 for details of structures **f** and **g**. Because the spin multiplicity is a doublet, the sum of the spin densities in the structures (except for the values in parentheses) is unity. Also see the footnote for Table 1. It was found that the spin density became localized at the Fe atom in structure **g** but localized at the substrate in structure **e**. [b] See the footnote for Table 1.

e. The activation energy for this reaction was only about 1 kcal/mol. From structure **g**, it is thought that the Fe−O1 bond is cleaved and that the monooxygenation reaction is completed. Although the SCRF calculations were carried out in a similar manner with the value of the dielectric constant set at 20, no significant differences were observed between the results of these calculations and those of calculations performed using a dielectric constant of 1.[45]

4. Conclusions

The substrate oxygenation mechanism by an ultimate species in monooxygenation by cytochrome P-450 (compound **I**) was investigated by the density functional theory method. The results of the calculation revealed that the substrate oxygenation mechanism consisted of four elementary processes, i.e., (1) formation of $[FeOH]^{3+}$ and a substrate radical by hydrogen atom abstraction from the substrate caused by $[FeO]^{3+}$, (2) rotation of the OH group of the sixth ligand of $[FeOH]^{3+}$ produced by process 1, (3) substrate radical binding with $[FeOH]^{3+}$, and (4) elimination of the oxygenated substrate formed at the sixth ligand binding site. The rate-determining step is process 1, hydrogen atom abstraction from the substrate, and the activation energy was determined to be about 15 kcal/mol. For this reason, it is thought that this reaction occurs in vivo.

Acknowledgment. The authors thank the Computer Center of the Institute for Molecular Science for the use of The NEC SX-5 computer. The computations were also carried out by the DRIA System at the Faculty of Pharmaceutical Sciences, Chiba University.

JA000908P